Fast Deposition of ZnS Thin Films by Intense Pulsed Ion Beam

Yutaka SHIMOTORI*, Meiso YOKOYAMA**, Shigetoshi HARADA*,
Katsumi MASUGATA* and Kiyoshi YATSUI*

A fast deposition technique has been novely developed for the preparation of ZnS thin films by use of an intense pulsed ion beam. The zinc and sulfur plasma have been produced by the irradiation of the intense pulsed beam (~6.6 GW/cm²) onto the surface of the ZnS target, which is deposited onto a substrate kept at room temperature. The temperature of the plasma has been evaluated to be ~ 1 eV. The deposition rate has been estimated to be ~ 2.3 cm/s, which is several orders of magnitude higher than those with any other methods. We have found that the films prepared have a polycrystalline hexagonal structure.

Key words: thin-film preparation/high-speed deposition/zinc sulfide/high-density, high-temperature plasma/intense pulsed ion beam

I. Introduction

An extremely high-power density of more than several GW/cm² can be easily concentrated using an intense pulsed ion beam[1)~3)]. Since the stopping range of the ions in a matter is very short, the surface of the target is instantaneously heated up to produce a high-density, high-temperature plasma, being expanded and deposited onto the substrate. Since the ions in such a plasma are expected to be very effective for the formation of well-condensed, high-crystalline thin films[4)], they can be used in the application for vacuum deposition[5)~7)]. Furthermore, the quick deposition of thin films might be expected. In this paper, we report the experimental results and the associated theoretical calculations on this new deposition technique for the preparation of ZnS thin films.

II. Experimental Arrangement

Figure 1 shows the cross-sectional view of the deposition system by the intense pulsed ion beam. The experiment has been carried out by using a pulse-power machine, "ETIGO-I"[2),3)] (1.2 MV, 240 kA, 0.3 TW, 50 ns, 14.4 kJ). The intense pulsed ion beam has been generated by a magnetically insulated diode (MID)[1)~3)]. The MID is constructed of a slab anode (Al) and a racetrack-shaped cathode (brass). A flashboard (polyethylene) has been attached to the surface of the anode as an ion source. The cathode works as an one-turn theta-pinch coil to produce a transverse magnetic field in the gap between the anode and cathode. To achieve the focusing of the beam geometrically, the part of the anode and cathode are shaped spherically (radius of the sphere is 160 mm and 150 mm for the anode and

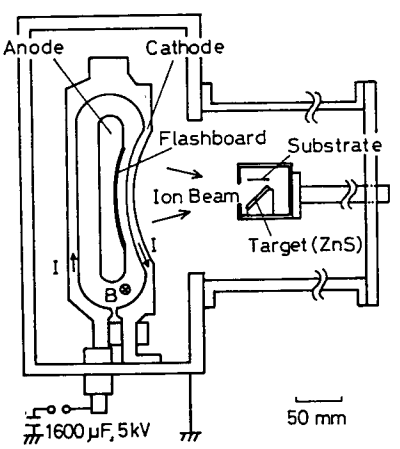

Fig. 1 Cross-sectional view of the deposition system by intense pulsed ion beam.

Received March 29, 1988.

* Laboratory of Beam Technology and Department of Electrical Engineering, NUT.
** Nippon Seiki Co. Ltd.

cathode, respectively). The gap length between the anode and cathode is 10 mm. The vacuum chamber has been evacuated to $\sim 10^{-4}$ Torr.

The target box in which the target and substrate are installed is located at $z = 130$ or 140 mm downstream from the anode. The diameter of the entrance is 9 or 20 mm. The sintered-ZnS target (35 mm in diameter) has been set on the stage which is inclined 45 degrees with respect to the axis of the beam. The distance from the entrance to the center of the target is 20 mm. Thus, the distance between the anode and target is 150 or 160 mm. The substrate of glass is located at $y = 16.5$ or 18 mm above the central line of the beam. The target and the substrate are kept at room temperature.

III. Experimental Results

a) *Waveforms*

Figure 2 shows the typical waveforms of a) inductively-calibrated diode voltage (V_d), b) diode current (I_d) and c) ion-current density (J_i) at $z = 140$ mm from the anode on the axis of the beam. From Fig. 2, we see $V_d \sim 940$ kV, $I_d \sim 60$ kA, $J_i \sim 7$ kA/cm^2 and τ (pulse width of J_i) ~ 30 ns (Full Width at Half Maximum, FWHM). From these results, the beam-power density can be estimated to be ~ 6.6 GW/cm^2 at the focusing point.

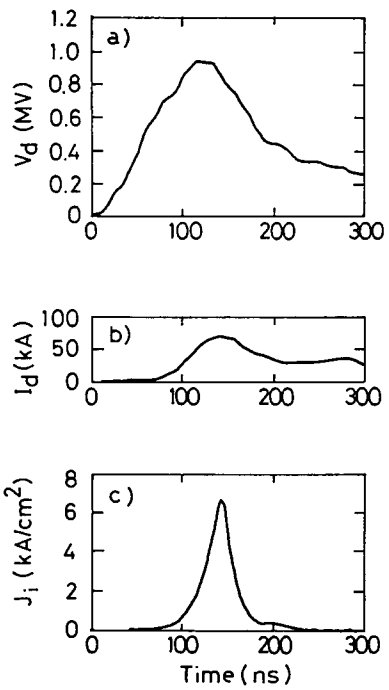

Fig. 2 Typical waveforms of the MID; a) diode voltage (V_d), b) diode current (I_d), c) ion-current density (J_i) measured at the focal point (z=140 mm).

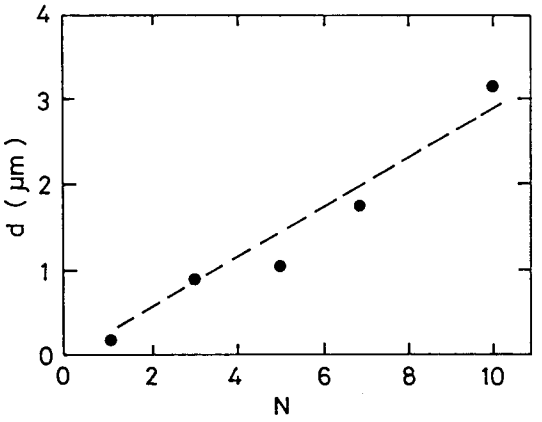

Fig. 3 Film thickness (d) on glass substrate plotted against number of shot (N).

b) *Thickness of Films*

Figure 3 shows the thickness (d) of the ZnS films prepared on the substrate plotted against the number of shot (N) of the beam. In this experiment, the entrance (9 mm in diameter) for the target box was located at $z = 140$ mm. The distance between the center of the target and the substrate was $y = 18$ mm. From Fig. 3, we see that the film thickness almost linearly increases with increasing the number of shot, and that the deposition rate of $\sim 0.3\,\mu$m/shot has been achieved.

c) *Crystallinity of Films*

Figure 4 shows an x-ray diffraction pattern (using Cu-K$_\alpha$ line) for the film prepared by one shot of the beam. In this experiment, the entrance (20 mm in diameter) of the target box was set at $z = 130$ mm. The distance from the target and the substrate was $y = 16.5$ mm. As seen from Fig. 4, a sharp peak which corresponds to the diffraction angle for the cubic (111) or the hexagonal (002) ZnS appears at $2\theta = 28.5°$. The other peak at $2\theta = 51.8°$ corresponds to the hexagonal (103) ZnS.

To clarify the structure of the films prepared, we have scraped the films to powder, and compared

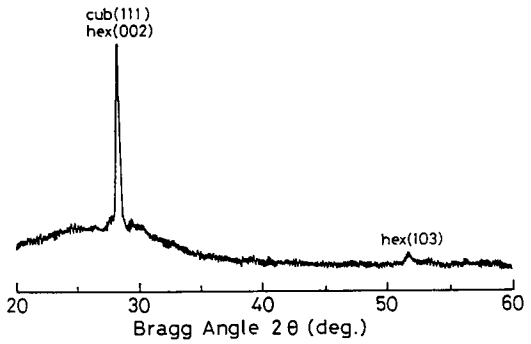

Fig. 4 X-ray diffraction pattern for ZnS thin film obtained on glass substrate kept at room temperature.

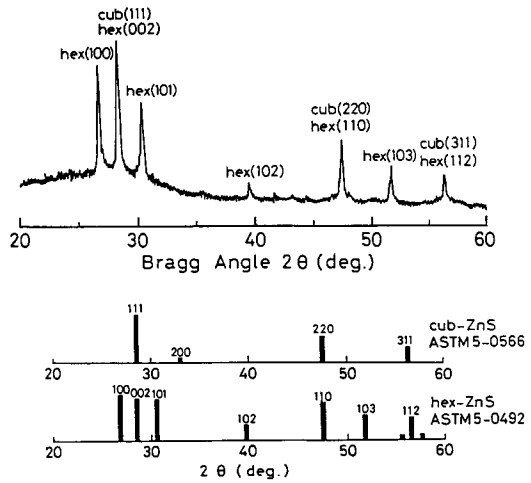

Fig. 5 X-ray diffraction pattern for ZnS powdered from thin film. Data are also referred from the ASTM for the powder of cubic- and hexagonal-ZnS.

with the x-ray diffraction pattern of ASTM (American Standard for Testing Materials) data for the powdered ZnS. Figure 5 shows the x-ray diffraction pattern measured for the ZnS powdered from thin films prepared in this experiment and the ASTM data of cubic- and hexagonal-ZnS. From Fig. 5, we have found that all the peaks are consistent to those for the hexagonal-ZnS of the ASTM data. From this comparison we have concluded that the films prepared have a hexagonal structure.

d) *Surface Structure of Target*

Figure 6 shows x-ray diffraction patterns for the surface of the ZnS target a) before and b) after the irradiation of the beam. As seen from Fig. 6, it is clear that the peaks for the cubic ZnS appear

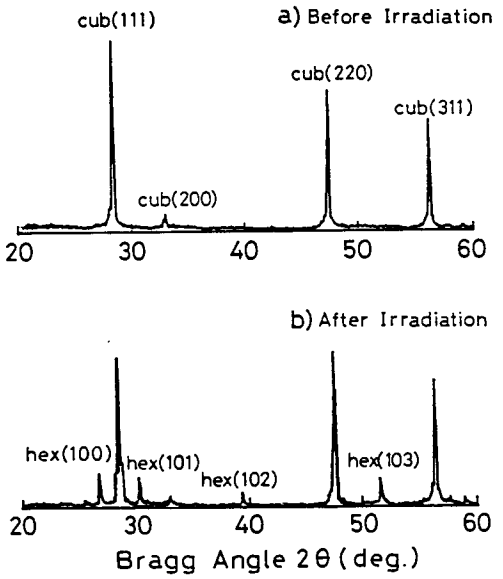

Fig. 6 X-ray diffraction patterns for the surface of sintered ZnS target, a) before and b) after the irradiation.

before the irradiation, and that several peaks for the hexagonal ones have grown after being irradiated by the beam. From these results, we have concluded that the surface of the ZnS target has been changed from the cubic- to the hexagonal-structure by the irradiation of the beam.

IV. Theoretical Calculations

a) *Temperature of Target*

From Fig. 2, we have estimated the energy of intense pulsed beam to be ~ 940 keV. Since the beam is mainly composed of protons[8], we have supposed all the ions are protons. From the stopping range for 940 keV protons in Al target (R_{Al}) of ~ 3.8 mg/cm^2,[9] we have calculated the range of protons in the ZnS target (R_{ZnS}) by Bragg-Kleeman rule[10] to be,

$$R_{ZnS} = (A_{ZnS}/A_{Al})^{1/2} \cdot R_{Al} \sim 5.2 \text{ (mg/cm}^2\text{)}.$$

Here, A_{Al} is the atomic weight of Al (= 27.0), and A_{ZnS} is the effective atomic weight for ZnS that is calculated as,

$$A_{ZnS} = ((A_{Zn} + A_S)/(A_{Zn}^{1/2} + A_S^{1/2}))^2 \sim 50.2,$$

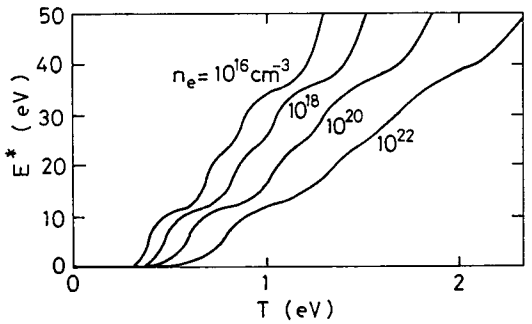

Fig. 7 Relationship between the mean energy injected to the atom of ZnS target (E*, summation of the ionization and thermal energy of plasma) and the temperature of the target plasma (T). Electron density (n_e) ranges from 10^{16} cm^{-3} to 10^{22} cm^{-3}.

where A_{Zn} and A_S are the atomic weight of Zn (= 65.4) and S (= 32.1), respectively.

Assuming the flat deposition profile in the ZnS target, energy density averaged in the surface of the ZnS target has been estimated to be,

$$940(\text{keV}) \times 7(\text{kA/cm}^2) \times 30(\text{ns})/5.2(\text{mg/cm}^2) \sim 3.8 \times 10^4(\text{J/g}).$$

Since the average mass of atoms in the target (m_{ZnS}) is 8×10^{-23} g, the mean energy deposited into each atoms of the target (E_{in}) has been calculated to be,

$$E_{in} \sim 3.8 \times 10^4(\text{J/g}) \times 8 \times 10^{-23}(\text{g})/1.6 \times 10^{-19}(\text{J/eV}) \sim 19(\text{eV}).$$

The thermal relaxation time between electrons and ions for the zinc and sulfur plasma (τ_{ei}) at temperature (T) ~ 1 eV and electron density (n_e) ~ 10^{20} cm^{-3} has been calculated to be,

$$\tau_{ei} \sim 2 \times 10^4 \cdot (T^{3/2}/n_e) \cdot (m_{ZnS}/m_e) \sim 18\ (\text{ps}),$$

where m_{ZnS} is the average mass of the target atom and m_e is the mass of an electron (~ 9.1×10^{-28} g). Since this relaxation time of ~ 18 ps is significantly shorter than the pulse width of the beam of ~ 30 ns, we suppose the temperature of the ions is equal to that of electrons.

Here, we consider that all energy deposited might be converted to the following:

(1) ionization energy,

(2) thermal energy of the ions and electrons in plasma,

(3) dissociation (ZnS → Zn+S) energy,

(4) vaporization energy.

Since the summation due to the processes (3) and (4) is estimated to be $E_h \sim 2.7$ eV[11], the specific energy of the plasma (E^*, the summation of (1) and (2)) is estimated to be,

$$E^* = E_{in} - E_h = 19 - 2.7 = 16.3\ (\text{eV}).$$

The relationship between E^* and the temperature of the plasma (T) have been calculated, and is plotted in Fig. 7. Assuming the electron density to be 10^{20} cm^{-3} from the previous experiment[12], we have estimated $T \sim 1$ eV for $E^* \sim 16.3$ eV.

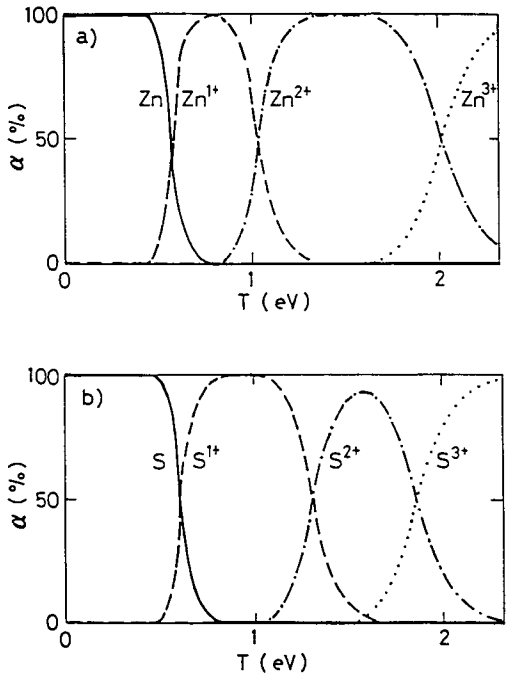

Fig. 8 Ionization ratio (α) for a) Zn and b) S atoms as a function of plasma temperature (T). Electron density is assumed to be 10^{20} cm^{-3}.

Figure 8 shows the ionization ratio (α) for a) Zn and b) S atoms as a function of the plasma temperature, which has been calculated by Saha's equation at electron density of ~ 10^{20} cm^{-3}. From Fig. 8, we see that at $T \sim 1$ eV the Zn atoms are singly or doubly ionized, and that the S atoms are singly ionized.

b) *Deposition Rate*

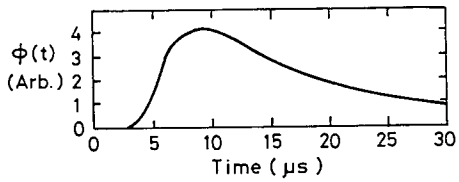

Fig. 9 Time variation of the flow rate of the ions (ϕ (t)) at the substrate (T = 1 eV, y = 18 mm).

By assuming that the velocity distribution of the ions evaporated from the surface of the target is three-dimensional Maxwellian, it may be possible to calculate the flow rate of the ions at the substrate. Figure 9 shows the flow rate of ions ($\phi(t)$) calculated at T = 1 eV and y (the distance between the target and the substrate) = 18 mm. If the effective deposition time has been evaluated by the FWHM of $\phi(t)$[13], the time has been calculated to be ~ 13.3 μs. From the experimental value of ~ 0.3 μm/shot and the calculated deposition time of ~ 13.3 μs, the deposition rate per second can be estimated to be,

0.3 (μm)/13.3 (μs) ~ 2.3 (cm/s).

Since the deposition rate for the conventional technique is known to be ~ 0.1 μm/s at the most, this method found here is significantly quick, being more than five orders of magnitude higher than those with any other technique.

V. Concluding Remarks

We have successfully prepared ZnS thin films for the first time by use of an intense pulsed ion beam. The deposition rate has been estimated to be ~ 2.3 cm/s, which is more than five orders of magnitude higher than those with any other technique. The temperature of the target plasma has been estimated to be ~ 1 eV, where the target atoms are singly or doubly ionized. The ZnS films prepared have a polycrystalline hexagonal structure.

With the extension of the studies above, it might be possible to make other types of thin films such as semiconductors, dielectric or magnetic materials, and superconductors very effectively.

Acknowledgements

The authors would like to thank Professor C.Y. Chang of National Cheng Kung University, Republic of China, and Mr. S. Ohta of Nippon Seiki Co., Ltd. for many valuable comments and discussions.

References

1) S. Humphries, Jr.: Nuclear Fusion, **20**, 1549 (1980).
2) K. Masugata, et al.: Jpn. J. Appl. Phys., **20**, L347 (1981).
3) K. Yatsui, A. Tokuchi, H. Tanaka, H. Ishizuka, A. Kawai, E. Sai, K. Masugata, M. Ito and M. Matsui: Laser and Particle Beams **3**, 119 (1985).
4) T. Takagi: J. Vac. Sci. Technol., **A2**, 382 (1984).
5) M. Yokoyama, Y. Shimotori, K. Masugata and K. Yatsui: *Proc. of World Conf. on Advanced Materials for Innovations in Energy, Transportation and Communications* (IUPAC, CHEMRAWN VI, Chem. Soc. Jpn., Tokyo), IA03 (1987).
6) Y. Shimotori, M. Yokoyama, H. Isobe, S. Harada, K. Masugata and K. Yatsui: J. Appl. Phys., **63**, 968 (1988).
7) Y. Shimotori, M. Yokoyama, S. Harada, K. Masugata and K. Yatsui: Oyo Buturi (Applied Physics in Japanese), **57**, 1078 (1988).
8) Y. Shimotori, K. Aga, K. Masugata, M. Ito, and K. Yatsui: *Proc. Top. Mtg. on Particle Beam Fusion and Its Related Problems*, edited by K. Niu, (Inst. of Plasma Phys., Nagoya Univ., Nagoya) IPPJ-769 (2), 267 (1986).
9) H.H. Andersen and J.F. Ziegler: "*Hydrogen Stopping Powers and Ranges in All Elements*", (Volume 3 of "The Stopping and Ranges of Ions in Matter," Pergamon Press, New York), p. 80 (1977).
10) R.D. Evans: "*The Atomic Nucleus*", (McGraw-Hill, New York), Chapt. 18-25 (1955).
11) I. Broser, et al.: "*Physics of II-VI and I-VII Compounds, Semimagnetic Semiconductors*", (Subvolume b, Volume 17 of the "LANDOLT-BORNSTEIN, Numerical Data and Functional Relationships in Science and Technology", ed. in chief: K. -H. Hellwege, Springer -Verlag Berlin, Heidelberg, New York, 1982).
12) From the measurement of ablation pressure (p) on aluminum target by using "ETIGO-I" (K. Yatsui et al.: Laser and Particle Beams **5**, 415 (1987)), we have estimated p ~ 5×10^8 Pa at beam power density of ~7 GW/cm^2. Using the relation of $p=(n_e+n_i)\,k_BT$, we thus evaluate n_e+n_i ~3×10^{20}cm^{-3} at T ~1 eV.
13) M. Hanabusa, M. Suzuki and S. Nishigaki: Appl. Phys. Lett., **38**, 385 (1981).